Integrated extended-cavity 1.5-μm semiconductor laser switchable between self- and anti-colliding pulse passive mode-locking configuration

Integrated Extended-Cavity 1.5-μm Semiconductor Laser Switchable Between Self- and Anti-Colliding Pulse Passive Mode-Locking Configuration

Valentina Moskalenko, Kevin A. Williams, and Erwin A. J. M. Bente, *Member, IEEE*

***Abstract*—We present the first integrated linear extended-cavity passively mode-locked (PML) semiconductor laser in which the operating mode can be switched electrically between two configurations. The first configuration is where the saturable absorber (SA) is located next to the output coupler, the so-called anti-colliding pulse mode-locking (ACPML) scheme. The second is where the SA is next to the high reflectance mirror, the self-colliding pulse mode-locking (SCPML) scheme. The 7.5-GHz PML was used to demonstrate experimentally the theoretical prediction that placing the SA next to the output coupler leads to a significant improvement in the laser stability and quality of the optical pulses. The experimental results show that the ACPML scheme allows for more deeply saturated SA due to the increase of optical power in the SA. The measurements of the RF spectra and autocorrelation traces confirm the superiority of the ACPML design in terms of pulse stability and width over the SCPML design for a wide range of operating conditions. The linewidth of the beat tone at the repetition rate was reduced by more than 60 times, the measured minimal autocorrelation width improved from 22 to 7.5 ps and a 3 dB increase in average output power was achieved.**

***Index Terms*—Mode-locked laser, quantum well laser, semiconductor laser, semiconductor laser, short pulse generation.**

I. Introduction

PASSIVE mode-locking is an important technique for the generation of short optical pulses and wide-band optical coherent combs. Uniquely, it does not require high frequency electronics to generate stable pulse trains. Semiconductor PMLs may find application in such areas as telecommunication [1], generation of microwave signals, sensing [2] and optical clock recovery [3]. PMLs do not require an external radio-frequency (RF) source and can be formed by a semiconductor optical amplifier (SOA) and a saturable absorber (SA) in a single waveguide Fabry–Perot cavity. The SOA provides optical gain which can be saturated at high optical powers. The SA provides amplitude modulation of the light inside the cavity through its saturation of absorption at lower intensities than the saturation of the SOA.

The combination of these two properties leads to the short optical pulse formation [4]. The simplicity of such circuits allows PMLs to be realized as a photonic integrated circuit (PIC) which may be combined with other optical elements into more complex systems. Due to their robustness, size and costs, integrated systems became a subject of interest, especially when active-passive integration technology is used.

However, there are a number of issues in realizing such integrated systems. One of them is the performance of semiconductor PMLs. The achieved optical pulses are typically longer than those obtained from solid state lasers, stable operation is limited to a narrow range of bias conditions and the pulse train exhibits a high level of amplitude and timing jitter. There are several highly relevant developments that are helping to bring this area forward. For instance it was shown that the introduction of gain-flattening filters into the laser cavity leads to shorter optical pulses and wider coherent combs [5], [6]. In order to stabilize the pulse train, RF or optical signals can be injected [7]. On the other hand, the performance of a PML can be improved in terms of both stability and the pulse characteristics by modifying the saturation energies of the SA and SOA [4]. Most literature reports on the so-called self-colliding pulse mode-locking (SCPM) scheme. This scheme is based on placing a short SA close at one end of the linear cavity and next to a high reflectivity mirror [8]–[10]. The high reflectivity mirror is typically a high reflection coated facet. The use of the high reflectivity mirror next to the SA is to optimize the power from the output facet. It also provides a deeper SA saturation due to the interaction of the pulse with itself inside the SA.

However in [11] it was shown theoretically that in an anti-colliding pulse mode-locking (ACPML) scheme, where the SA is placed next to the low reflectivity output coupler (OC) mirror, a weaker saturation of the gain in the SOA and a more deeply saturated absorption in the SA can be achieved. The study was presented as a comparison of three configurations: ACPML, SCPML and symmetrical mode-locking (SML). SML configuration is where the SA is placed at the one end and reflectivities of both cavity ends were chosen equal. The study in [11] showed that the ACPML configuration leads to an enlargement of the operating current range, a reduction of amplitude and timing jitter, an increase of optical power and a reduction of pulse duration in comparison with the other two configurations.

Recently in [12] an experimental study of a laser in the ACPML configuration (one high reflectivity and one low reflectivity mirror) and in the SML configuration (both mirrors with the same reflectivity), was presented. The performance of an uncoated Fabry–Perot two-section mode-locked laser at 1.5 μm was compared before (30% reflectivity on both sides)

Manuscript received February 1, 2015; revised May 18, 2015 and March 13, 2015; accepted May 18, 2015. This work was supported by European Community's Seventh Framework Program FP7/2007-2013 under Grant 257210 PARADIGM.

The authors are with the Department of Electrical Engineering, Eindhoven University of Technology, Eindhoven, MB 5600, The Netherlands (e-mail: v.moskalenko@tue.nl; k.a.williams@tue.nl; e.a.j.m.bente@tue.nl).

Color versions of one or more of the figures in this paper are available online at http://ieeexplore.ieee.org.

Digital Object Identifier 10.1109/JSTQE.2015.2435900

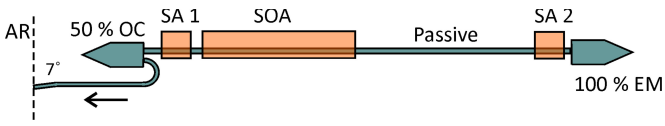

Fig. 1. Sketch of linear passive mode-locked laser. MIRs were used as an OC and EM. Three active sections (orange) were positioned in the way that colliding and anti-colliding designs were realized.

and after applying a low reflection coating (10% reflectivity) to the SA facet and a high reflection coating (over 90% reflectivity) to the other facet. A reduction of the amplitude and timing jitter, an increase of the operating range of bias conditions and an increase of the pulse power was achieved. In this work it was observed that the peak emission of the coated laser had shifted significantly. According to the authors this could be caused by the spectral filtering introduced by the coating.

However, as it was discussed above, much experimental and theoretical work was done on linear PMLs using the SCPML configuration, where one facet has 100% reflectivity in order to decrease intracavity loss. In this work we present an experimental study of an InP-based quantum well integrated PMLL with an extended linear cavity in ACPML and SCPML configurations. Preliminary results were published in [13]. Moreover, the laser design allows to realize both configurations by using three separate active sections with quantum wells as well as passive integrated wavelength-independent mirror structures thus avoiding the use of coatings. The use of passive mirror structures in an active-passive integration scheme allows for a precise control of the SA length since cleaving inaccuracies are avoided [14]. In this case the PMLL can be freely located on the chip for further integration. In this paper we qualitatively verify the theoretical predictions and show significant improvement of the stability, optical power, pulse duration and enlargement of the operating condition range of a PML in the ACPML configuration in comparison to one in SCPML configuration.

II. Experimental Results

A. Linear Mode-Locked Laser Geometry

In this work we present an extended cavity linear laser design which includes a SOA, a SA as well as passive waveguides and mirror structures. The laser was designed as an InP PIC using a library of standardized building blocks and fabricated within a multiproject wafer run available through an Oclaro foundry service [15].

A schematic sketch of the linear PMLL are shown in Fig. 1(a). The repetition rate is determined by the total length of the cavity. In the case of low repetition rates, the use of passive waveguides helps to reduce self-phase modulation effects caused by propagation of the light through the active sections. The laser presented here consists of three active sections (SA1, SOA and SA2), a passive waveguide section and multimode interference reflectors (MIR). In order to be used as OC and end mirror (EM), the 107 μm long MIRs [16] were designed to provide 50% and 100% respectively. However, in reality fabrication imperfections cause a power loss of less than 1 dB (20%) for one-port MIR (EM) and 1.4 dB (28%) for two-ports MIR (OC). The total length of the cavity including both MIRs is 5.5 mm.

The finite length of the mirrors can significantly reduce the pulse interaction with its reflection within the SA. In [17] it was shown theoretically that an increase of the distance between the SA and a flat OC mirror (e.g., a facet mirror) ultimately leads to a reduction of pulse energy and a decrease in stability of the pulse train in the anti-colliding configuration. Increase of the distance between SA and the flat mirror also broadens the optical pulses. However stable mode-locked operation can be obtained when the distance between the SA and OC mirror is up to four times of the length of the SA and this distance does not exceed the spatial width of the pulse. In was shown that under these conditions the PML realized in the ACPML configuration features better performance than the one in the SCPML configuration.

To minimize possible back reflections from the edges of the chip the output waveguide was 7° tilted with respect to the cleaved and AR-coated facet. The ring waveguide attached to the 50% MIR output has 150 μm radius. All active sections SA1, SA2 and the SOA are electrically isolated. By applying various biasing conditions on SA1 and SA2 we can locate the SA near the EM or near the OC. When SA1 is reversely biased and the same current density is applied on SOA and SA2 the SA is positioned near the OC and an ACPML configuration is realized. An SCPML configuration can be achieved by applying the same forward bias current density to SA1 and SOA and a reverse bias voltage on SA2. The cavity included SOA section of length 2 mm, two absorbers SA1 and SA2 of length 100 μm. The total length of the cavity is 5.5 mm. The active sections were all based on the same InGaAsP multi-quantum well core.

B. Optical Power Characteristics

The chip was mounted on a copper chuck that was temperature stabilized at 18 °C. The light from the waveguide connected to the OC was collected using a lensed fiber with anti-reflection coating. In order to prevent back-reflections to the chip from optical equipment connected to the fiber an optical isolator was used. To investigate the influence of the position of the SA on the energy emitted by the laser and the energy inside the SA, we measured the output optical power and the photocurrent generated in the SA as a function of the current injected in the SOA. The output optical power was measured after a 50% splitter. The generated photocurrent in the SA is a measure of the power at that point in the cavity at the fixed applied voltage. Fig. 2 shows both these dependencies for the ACPML (black curves) and for the SCPML (red curve) for different values of absorber bias. Notice, that the fibre coupled power levels in both configurations are relatively low compared to other monolithic PMLs [9], [12]. In addition to the coupling losses (5 dB) the PML exhibits significant intracavity losses due to an error in the fabrication. The laser was fabricated in non-commercial experimental foundry run, which had non-typical waveguide losses of 14 dB/cm.

The small spikes on the curves are related to the change in the laser dynamic regimes, which are represented with dashed

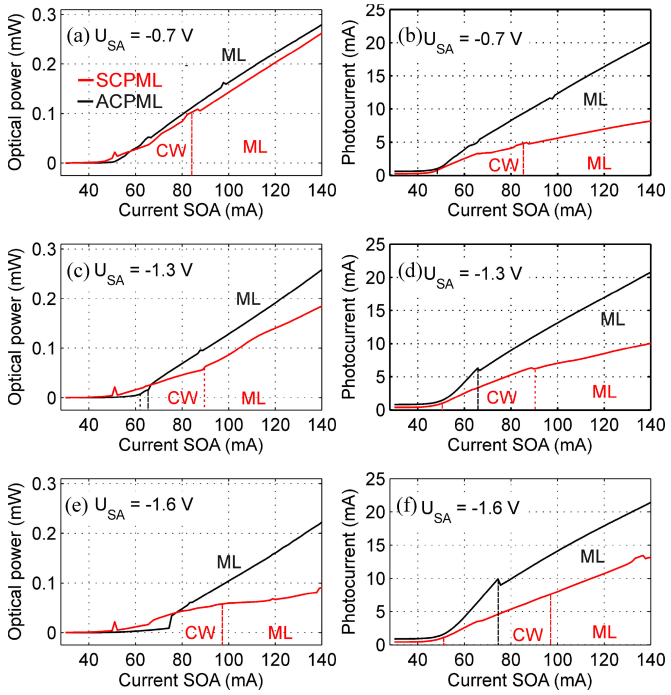

Fig. 2. (a), (c), and (e) Shows dependencies of fiber-coupled optical power on the current injected in SOA for three different voltages applied on SA in ACPML (black curve) and SCPML (red curve) configurations. (b), (d), and (f) Shows photocurrent generated in SA for both configurations as a function of the current injected in SOA section.

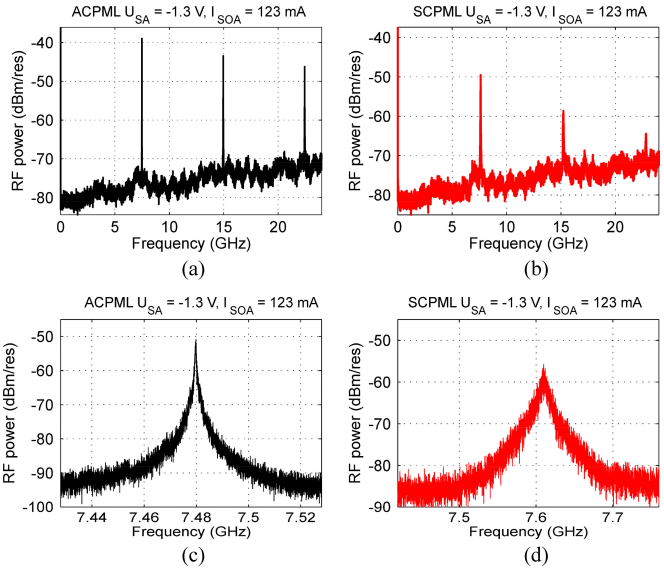

Fig. 3. (a) and (b) Shows RF beat signal produced on a fast photodiode and recorded with electrical spectrum analyzer recorded at $U_{\mathrm{SA}} = -1.3$ V and $I_{\mathrm{SOA}} = 123$ mA for ACPML and SCPML respectively. (c) and (d) shows detailed view of the spectra recorded at the same operating conditions as shown in (a) and (b) with resolution bandwidth of 20 and 200 kHz respectively.

lines on Fig. 2(b), (d), (f). At a low bias voltage U_{SA} the optical power dependencies for both configurations show almost the same slope. However, with increasing U_{SA} the optical power coupled from the SCPML configuration drops with respect to that of the ACPML configuration. The linear absorption in the SA will increase with increasing U_{SA}. Thus the reduction in output power of the SCPML configuration with respect to the ACPML configuration is related to a less saturated SA in the SCPML compared to the ACPML. The reason for that is that the highest pulse energy is available near the OC. Fig. 2(b), (d), (f) shows that indeed the optical power level in the SA in the ACPML is much higher than those measured for the SCPML. Notice that in both configurations an increase of U_{SA} leads to an increase of the photocurrent in the SA. The dark current was in the order of few nanoampere. However, this effect is more pronounced in the case of the SCPML configuration, due to its less saturated SA. In the ACPML configuration the value of photocurrent at $I_{\mathrm{SOA}} = 140$ mA changes from 20.15 to 21.41 mA with increasing U_{SA} whereas in the case of the SCPML configuration the photocurrent at the same I_{SOA} value increases from 8.17 to 13.1 mA. The laser in the SCPML configuration operates in continuous wave (CW) regime for low I_{SOA} since the SA is not sufficiently saturated at those current levels. With increasing I_{SOA} the laser enters a mode-locked regime.

These observations fully confirm the theoretical prediction of the increase of output power and the optical power inside the SA in the case of an ACPML design. The higher level of photocurrent generated in the SA in the case of an ACPML is a result of less saturated SOA, which in principle should lead to the reduction of self-phase modulation effects and a more stable pulse train [10]. In the next section we present the evaluation of the influence of the position of the SA on PML stability.

C. *Stability and Pulse Quality Characterization*

In [10] it was shown that theoretically the use of an ACPML scheme leads to the reduction of amplitude and timing jitter over a large range of the injected SOA current for a fixed reverse bias voltage on the SA. However it is also relevant to consider the effect of varying the SA bias voltage. Variation of this bias voltage leads to a change in the SA recovery time and in the SA absorption spectrum. This in turn influences the output properties of the laser [14]. In this section we present an experimental comparison of the timing stability and pulse duration for the two configurations over a range of U_{SA} and I_{SOA}. The influence of the SA position on the stability was evaluated by performing spectral measurements of RF beat tones that were generated in a 50 GHz photodiode and recorded using a 50 GHz electrical spectrum analyzer. For the several operating conditions the measurements of optical spectra were performed using high-resolution optical spectrum analyzer. The electrical spectrum for the ACPML configuration recorded at $U_{\mathrm{SA}} = -1.3$ V and $I_{\mathrm{SOA}} = 123$ mA shows a peak at the fundamental frequency and second and third harmonics (see Fig. 3(a)). Fig. 3(b) presents a RF spectrum of the PMLL in SCPML configuration recorded at the same operating conditions as in Fig. 3(a). Fig. 3(a) shows a stronger fundamental tone and its higher order overtones in comparison with the spectrum presented in Fig. 3(b). Fig. 3(c), and (d) shows more detailed RF spectra around the fundamental peaks for the both configurations. The –10 dB linewidth of the RF peak depicted in Fig. 3(a) is 1.4 and 23 MHz in Fig. 3(b). Even though in this study for both the ACPML and SCPML

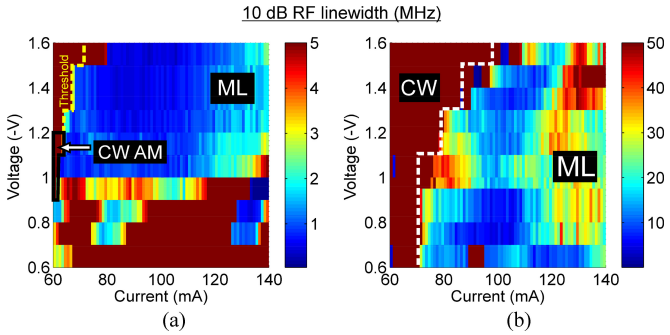

Fig. 4. The map of the RF linewidth measured at –10 dB level below the peak for the case of (a) ACPML and (b) SCPML design.

configurations the same device was used, the fundamental frequency of the two configurations differs by more than 100 MHz. In [9] it was shown that such a large detuning from the cavity's roundtrip originates from saturation effects in the SOA and SA sections and can vary with the optical pulse intensity. The Fig. 3(c) shows a reduction of the linewidth of the fundamental peak when the ACPML configuration is used. This indicates a lower level of timing jitter [19].

In order to compare two designs in terms of timing jitter for wide range of operating conditions, the linewidth of the fundamental peak at the –10 dB level was measured. Fig. 4(a) and (b) shows maps of the RF peak linewidth for the ACPML and SCPML configurations respectively. Please notice that the colour scale for the linewidth in Fig. 4(a) is ten times larger than the scale used in Fig. 4(b). Depending on the operating conditions, various dynamical regimes were observed in both configurations. In the narrow range of currents (1–2 mA) just above the threshold, the laser in the ACMPL configuration exhibits CW regime with amplitude instabilities. This range is indicated by the black solid line in Fig. 4(b). A further increase of the current leads to a buildup of the mode-locking state. In the case of the SCPML configuration the laser first enters CW state due to the low optical power in the SA. Then with increasing injection current the laser proceeds to a mode-locked state. This was confirmed by the measurements of the optical spectra. From these graphs it clearly appears that for a large range of operating conditions the RF linewidth of the laser in ACPML configuration is significantly decreased in comparison to the other configuration.

The minimum observed linewidth at –10 dB level for the ACPML configuration was 36 KHz, whereas for the SCPML it was 2.4 MHz. Therefore, these investigations confirm that the use of an ACMPL design leads to a significant reduction of the timing jitter and enlargement of the region of stable mode-locking.

The amplitude noise can be evaluated through the analyzing of the RF signal at low frequencies. In [12] it was shown that the PML realized in the ACPML configuration exhibited suppressed amplitude noise levels when compared with the SCPM case. However, in our case the low frequency components were not observed above the system noise floor of –80 dBm in the mode-locking state for both configurations.

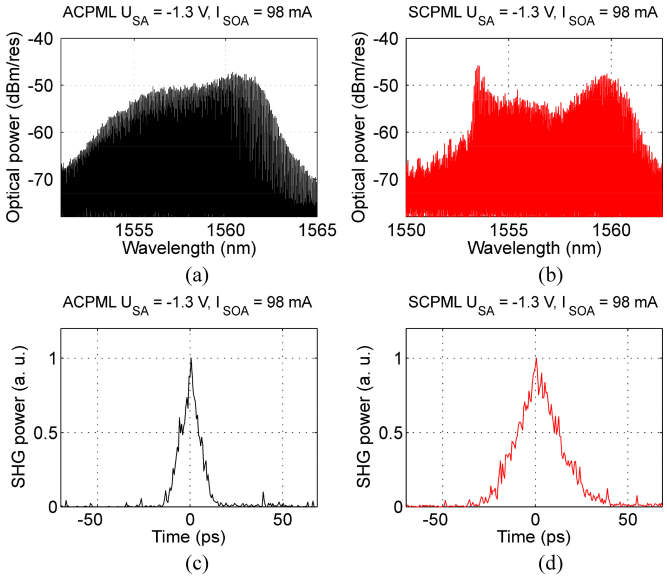

Fig. 5. AC traces recorded at $U_{\mathrm{SA}} = -1.3$ V and $I_{\mathrm{SOA}} = 98$ mA for the (a) ACPML and at for (b) SCPML configurations. (c) and (d) Show optical spectra measured for the same operating conditions as (a) and (b) for the ACPML and SCPML respectively.

To investigate the influence of the position of the SA on the output pulse shape in the time domain, second harmonic autocorrelation (AC) intensity profiles were measured using an autocorrelator in a background free configuration. Since the output power from the lasers was quite low, the signal was first amplified by a low noise erbium doped fiber amplifier (EDFA) and then sent through the polarization controller to the autocorrelator. The length of the erbium doped fiber was 42 m with dispersion parameter of 10.8 ps/(nm·km). More details of the influence of dispersion and non-uniform amplification caused by the EDFA on the AC trace can be found in [20].

The Fig. 5 shows an example of optical spectra and AC traces for the ACPML (see Fig. 5(a) and (c)) and the SCPML (see Fig. 5(b) and (d)). Both spectra and AC traces were recorded at $U_{\mathrm{SA}} = -1.3$ V and $I_{\mathrm{SOA}} = 98$ mA. Optical spectra for both configurations are centered around 1557 nm. The optical comb presented in Fig. 5(a) features a bandwidth of 4.6 nm full-width at half-maximum (FWHM), whereas the optical spectrum in Fig. 5(b) is 0.4 nm wide. Such a narrow bandwidth measured at 3 dB level in the case of SCPML configuration is caused by the non-uniform shape of the spectrum. This spectrum shows two pronounced maxima around 1554 and 1560 nm, which were present over the whole range of injected currents in mode-locking regime. The reason of this is not yet understood and requires further investigation. The measurements of the AC traces confirm the coherency between longitudinal modes in mode-locked state. AC trace background level suppression of more than 30 times was observed in the transition between CW to mode-locked state. This means that in the mode-locked state most of the power is concentrated in the optical pulse. The width of the AC measured at the level of half maximum (FWHM) was 9.7 ps for the ACPML configuration and 21.8 ps for SCPML configuration. It should be noted that for both configuration the optical pulses are expected to have a significant amount of chirp.

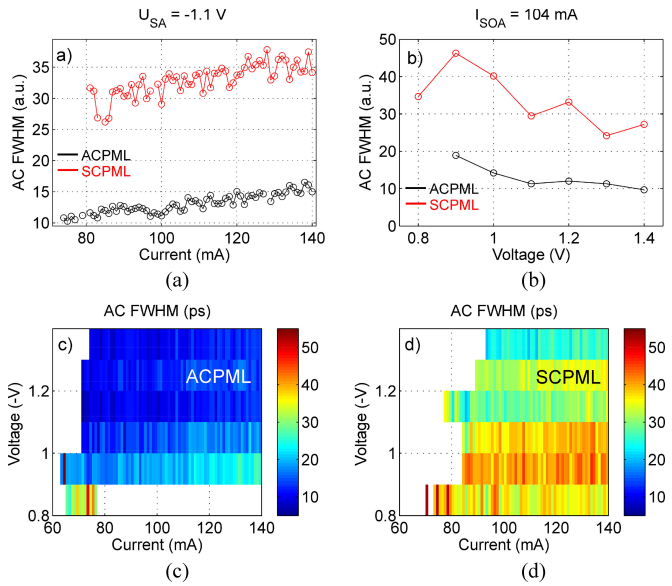

Fig. 6. (a) FWHM as a function of injected current at $U_{\mathrm{SA}} = -1.1$ V. (b) FWHM dependence on applied voltage at $I_{\mathrm{SOA}} = 104$ mA. Both (a) and (b) dependencies were measured for ACPML (black) and SCPML (red) configurations. The map of the AC width (FWHM) for the ACPML (c) and SCPML configurations (d) as a function of total forward bias current and reverse bias voltage.

The FWHM of AC traces was chosen as a characteristic of the time domain PML performance. AC traces were measured for the same operating points as in the RF measurements. All time traces were obtained for the same autocorrelator settings of 150 ps scan range with 260 data points, which correspond to a 580 fs time resolution in the AC signal. The FWHM of AC was chosen as a characteristic of the time domain PML performance. Fig. 6(a) shows the dependence of the FWHM of the AC traces on injected current at fixed $U_{\mathrm{SA}} = -1.1$ V for the ACPML (red) and SCPML (black) configurations. In both cases the increase of injected current leads to the broadening of the pulses due to the increase in self-phase modulation effects. When varying the voltage applied on the SA at fixed current on the SOA ($I_{\mathrm{SOA}} = 104$ mA), both configurations show a decrease of the FWHM with U_{SA}, which is attributed to a reduction of SA recovery time.

Fig. 6(c) and (d) shows the AC FWHM as a function of injected current and applied voltage for the ACPML and SCPML designs. Pulse formation was observed in the regions indicated in the contour plot where the color indicates the AC FWHM. The AC FWHM is varying between 7.5 and 50 ps. In both configurations the PML features relatively broad optical pulses in comparison with other results obtained from integrated QW PMLs [12], [14], [20]. This can be caused by the reduction of pulse interaction with its reflection in the SA due to the use of finite mirror length. The energy inside SA is also reduced in both cases due to the high losses in passive waveguide, which can lead to the broadening of the pulse.

The maps AC FWHM indicate a significant reduction of the pulse width over whole range of operating conditions when the ACPML design is used. In this case the minimum achieved AC width was 7.5 ps, whereas the minimum width in the SCPML configuration was 22 ps. Combining these results with the results achieved from the optical power measurements we can conclude that in an ACPML configuration the peak power of the pulse is increased by more than 4 times at the high applied voltages in comparison with the SCPML configuration.

III. Conclusion

In this work we experimentally investigated the performance of a linear semiconductor passively mode-locked laser that can be switched between the ACPML and SCPML configurations. The design of the PML that was realized allowed for both configurations to be evaluated using the same device. As was predicted in [11], the placing of the SA next to the low reflectivity mirror leads to an increase of output power up to two times in comparison with the configuration where the SA is placed at the high reflectivity mirror. By measuring the photocurrent generated in the SA it was shown that the modulation of the SA is enhanced in the ACMPL design. Observation of RF spectra showed that in the ACMPL design the RF peak linewidth is decreased for a wide range of the current injected in the SOA and voltage applied on the SA. This indicates the reduction of timing jitter and increase of the region of stable mode-locked operation. The analysis of AC traces shows that a minimum AC pulse width reduces from 22 to 7.5 ps. These results fully confirm the theoretical prediction made in [11] of the superiority of the ACMPL design over SMPL design.

References

[1] Y. Ben M'Sallem *et al.*, "Quantum-dash mode-locked laser as a Source for 56-Gb/s DQPSK modulation in WDM multicast applications," *IEEE Photon. Technol. Lett.*, vol. 23, no. 7, pp. 453–455, Apr. 2011.

[2] J. Mandon, G. Guelachvili, and N. Picqué, "Fourier transform spectroscopy with a laser frequency comb," *Nature Photon.*, vol. 3, no. 2, pp. 99–102, Feb. 2009.

[3] T. Ohno *et al.*, "Recovery of 160 GHz optical clock from 160 GBit/s data stream using modelocked laser diode," *Electron. Lett.*, vol. 40, no. 4, pp. 1–2, Feb. 2004.

[4] H. A. Haus, "Mode-locking of lasers," *IEEE J. Sel. Topics Quantum Electron.*, vol. 6, no. 6, pp. 1173–1185, Nov. 2000.

[5] V. Moskalenko, J. Javaloyes, S. Balle, M. K. Smit, and E. A. J. M. Bente, "Theoretical study of colliding pulse passively mode-locked semiconductor ring lasers with an intracavity Mach-Zehnder modulator," *IEEE J. Quantum Electron.*, vol. 50, no. 6, pp. 415–422, Jun. 2014.

[6] J. S. Parker *et al.*, "Theory and design of THz intracavity gain-flattened filters for monolithically integrated mode-locked lasers," *IEEE J. Quantum Electron.*, vol. 48, no. 2, pp. 114 –122, Feb. 2012.

[7] E. Sooudi *et al.*, "A novel scheme for two-level stabilization of semiconductor mode-locked lasers using simultaneous optical injection and optical feedback," *IEEE J. Sel. Topics Quantum Electron.*, vol. 19, no. 4, art. no. 1101208, Jul. 2013.

[8] Y. Barbarin, E. A. J. M. Bente, M. J. R. Heck, Y. S. Oei, R. Nötzel, and M. K. Smit, "Characterization of a 15 GHz integrated bulk InGaAsP passively modelocked ring laser at 1.53μm," *Opt. Exp.*, vol. 14, pp. 9716–9727, 2006.

[9] S. Arahira and Y. Ogawa, "Repetition-frequency tuning of monolithic passively mode-locked semiconductor lasers with integrated extended cavities," *IEEE J. Quantum Electron.*, vol. 33, no. 2, pp. 255–264, Feb. 1997.

[10] M. G. Thompson, A. Rae, M. Xia, R. V. Penty, and I. White, "InGaAs quantum-dot mode-locked laser diodes," *IEEE J. Sel. Topics Quantum Electron.*, vol. 15, no. 3, pp. 661–672, May 2009.

[11] J. Javaloyes and S. Balle, "Anticolliding design for monolithic passively mode-locked semiconductor lasers," *Opt. Lett.*, vol. 36, no. 22, pp. 4407–4409, Nov. 2011.
[12] J.-P. Zhuang, V. Pusino, D. Ying, S.-C. Chan, and M. Sorel, "Experimental investigation on anticolliding-pulse mode-locked semiconductor lasers," *Opt. Lett.*, vol. 40, no. 4, pp. 617–620, Feb. 2015.
[13] V. Moskalenko, V. Anand, M. Smit, K. Williams, and E. Bente, "Experimental study of the stability of a linear passively mode-locked laser," in *Proc. IEEE Photonics Soc. Symp.*, Enschede, The Netherlands, 2014, pp. 115–118.
[14] C. Gordón, R. Guzmán, X. Leijtens, and G. Carpintero, "On-chip mode-locked laser diode structure using multimode interference reflectors," *Photon. Res.*, vol. 3, no. 1, pp. 15–18, Feb. 2015.
[15] M. Smit *et al.*, "Generic foundry model for InP-based photonics," *IET Optoelectron.*, vol. 5, no. 5, pp. 187–194, Oct. 2011.
[16] E. Kleijn, M. K. Smit, and X. J. M. Leijtens, "Multimode interference reflectors: A new class of components for photonic integrated circuits," *J. Lightw. Technol.*, vol. 31, no. 18, pp. 3055–3063, Sep. 2013.
[17] V. Moskalenko, A. Pellacani, J. Javaloyes, M. Smit, and E. Bente, "Design of monolithically integrated InGaAsP/InP passively-modelocked linear quantum well lasers in an active-passive integration scheme," in *Proc. IEEE Photon. Soc. Symp.*, 2012, pp. 283–286.
[18] J. Javaloyes and S. Balle, "Mode-locking in semiconductor Fabry-Perot lasers," *IEEE J. Quantum Electron.*, vol. 46, no. 7, pp. 1023–1030, Jul. 2010.
[19] F. Kefelian, S. O'Donoghue, M. T. Todaro, J. G. McInerney, and G. Huyet, "RF linewidth in monolithic passively mode-locked semiconductor laser," *IEEE Photon. Technol. Lett.*, vol. 20, no. 16, pp. 1405–1407, Aug. 2008.
[20] V. Moskalenko *et al.*, "Record bandwidth and sub-picosecond pulses from a monolithically integrated mode-locked quantum well ring laser," *Opt. Exp.*, vol. 22, no. 23, pp. 28865–28874, Nov. 2014.

Valentina Moskalenko was born in Donetsk, Ukraine. She received the M.Sc. degree in physics from Lomonosov State University, Moscow, Russia. She joined the Eindhoven University of Technology, Eindhoven, The Netherlands, in 2011, where she is currently working toward the Ph.D. degree. Her current research interests include photonic integrated circuits in InP and semiconductor short-pulse laser systems.

Kevin A. Williams received the B.Eng. degree from the University of Sheffield, Sheffield, U.K., in 1991, and the Ph.D. degree from the University of Bath, Bath, U.K., in 1995. He moved to the University of Cambridge, Cambridge, U.K., in 2001, and was elected as a Fellow at Churchill College, Cambridge. He currently leads the Photonic Integration Group. He received a Royal Society University Research Fellowship at the University of Bristol, Bristol, U.K., in 1996. In 2006, he became the European Commission Marie Curie Chair at the Eindhoven University of Technology, The Netherlands. In 2011, he received the Vici Award from the Netherlands Organization for Scientific Research.

Erwin A. J. M. Bente (M'01) received the M.Sc. degree in physics and the Ph.D. degree from Vrije Universiteit, Amsterdam, The Netherlands, in 1983 and 1989, respectively. From 1988 to 1994, he was with Urenco Nederland B.V. and led a research group on laser isotope separation. From 1994 to 1996, he was a Researcher with Vrije Universiteit, where he worked on solid-state coherent light sources and isotope separation of stable isotopes. He was a Research Team Leader at the Institute of Photonics, University of Strathclyde, Glasgow, U.K., and was involved in high-power diode-pumped solid-state lasers, passive mode-locking, and femtosecond laser machining. Since 2001, he has been an Associate Professor at the Communication Technology: Basic Research and Applications Research Institute, Eindhoven University of Technology, Eindhoven, The Netherlands, where he is involved in integrated semiconductor laser systems.